Microstructure and hyperfine interactions of the $Fe_{73.5}Nb_{4.5}Cr_5CuB_{16}$ nanocrystalline alloys: Mössbauer effect temperature measurements

1998 J. Phys.: Condens. Matter 10 3159

(http://iopscience.iop.org/0953-8984/10/14/006)

J. Phys.: Condens. Matter **10** (1998) 3159–3176. Printed in the UK PII: S0953-8984(98)88668-2

Microstructure and hyperfine interactions of the $Fe_{73.5}Nb_{4.5}Cr_5CuB_{16}$ nanocrystalline alloys: Mössbauer effect temperature measurements

M Miglierini†§, I Škorvánek‡ and J M Grenèche§

† Department of Nuclear Physics and Technology, Slovak University of Technology, Ilkovičova 3, 812 19 Bratislava, Slovakia

‡ Institute of Experimental Physics, Slovak Academy of Sciences, Watsonova 47, 043 53 Košice, Slovakia

§ Laboratoire de Physique de l'Etat Condensé, UPRESA CNRS 6087, Université du Maine, Faculté des Sciences, 72085 Le Mans Cédex 9, France

Received 23 October 1997, in final form 21 January 1998

Abstract. Mössbauer spectrometry, magnetization measurements and differential scanning calorimetry were used to investigate the microstructure and hyperfine interactions in the $Fe_{73.5}Nb_{4.5}Cr_5CuB_{16}$ nanocrystalline alloy obtained by heat treatment of the original amorphous precursor at the temperature of 550 °C for 1 hour. ^{57}Fe transmission Mössbauer spectra were taken in the temperature range 5–475 K without and with external magnetic field oriented parallel ($H_{ext} \approx 0.05$ T) and perpendicular ($H_{ext} \approx 4$ T) to the ribbon-shaped sample. The as-quenched state of the alloy was also investigated. The Mössbauer effect measurements confirmed the presence of α-Fe phase upon nanocrystallization. Magnetic states of Fe atoms in amorphous and interfacial regions are studied via distributions of hyperfine fields.

1. Introduction

Soft magnetic properties of some nanocrystalline alloys like FeNbCuSiB [1] or FeM(Cu)B [2, 3] provide a strong support for many a practical application [4]. As a result, nanocrystalline materials prepared by partial crystallization of metallic glasses stand in the centre of research activities both for scientific and technological reasons. To understand fully the origin of their unique properties, specific tools for structural and/or magnetic studies on an atomic scale, comprising nuclear probe methods, should be employed [5].

In most nanocrystalline alloys x-ray diffraction may yield an estimate of average crystal size and the nature of crystalline phases, whereas the information about the amorphous residual matrix is very limited. ^{57}Fe Mössbauer spectrometry permits us to probe immediate surroundings of resonating iron nuclei located in different structural positions. The refinement of spectral parameters, however, is often a difficult task because Mössbauer spectra of nanocrystalline materials consist, in general, of two superimposing components originating from the nanocrystallites and from the amorphous matrix whose hyperfine characteristics are quite similar. In order to separate these two components, one usually modifies the starting amorphous composition by adding chromium which lowers the Curie temperature and, consequently, separates the hyperfine interactions inside the nanocrystals and the amorphous remainder.

0953-8984/98/143159+18$19.50

Microstructure and magnetic properties of nanocrystals and of amorphous matrix were studied for the $Fe_{66}Cr_8CuNb_3Si_{13}B_9$ nanocrystalline alloy by x-ray diffraction, differential thermal analysis, transmission electron microscopy (TEM) and magnetization measurements [6] and Mössbauer spectrometry [7, 8], respectively. A similar system of nanocrystalline $Fe_{73.5-x}Cr_xCuNb_3Si_{13.5}B_9$ ($0 \leqslant x \leqslant 5$) alloys was investigated by differential scanning calorimetry (DSC), TEM and thermomagnetic measurements [9]. Chromium redistribution out of the nanocrystalline grains was reported [7] whereas the thermomagnetic studies [9] indicate that some minor population of Cr that exhibits a limited solubility in α-Fe,Si can be present also in the nanocrystalline phase.

In Si-containing nanocrystalline alloys, the complexity of the hyperfine structure of Mössbauer spectra, which is due to the presence of many non-equivalent iron sites in the bcc FeSi crystalline phase, prevents a detailed analysis of the intergranular phase [10]. The latter plays an important role in the magnetic behaviour of the nanocrystalline systems by transmitting ferromagnetic exchange coupling among adjacent crystalline grains through the amorphous matrix [11, 12]. This phenomenon can be precisely studied only for Mössbauer spectra with one crystalline site of a bcc Fe phase, e.g. FeZr(Cu)B [13], FeTiCuB [14] or FeNbCrCuB [15].

In the present paper we report on the magnetic microstructure within the $Fe_{73.5}Nb_{4.5}Cr_5CuB_{16}$ nanocrystalline alloy. Our attention is focused on temperature dependence of hyperfine interactions investigated predominantly by Mössbauer spectrometry to demonstrate its power and abilities in the investigation of nanocomposite materials. The recently introduced fitting procedure based on two independently refined distributions of hyperfine fields and separate discrete spectral components [16] improves the diagnostic potential of Mössbauer spectra and makes the analysis of the amorphous residual matrix, the interface zone and the crystalline phase more accurate [17]. Moreover, addition of 5% Cr to the master Fe–Nb–Cu–B alloy decreases the Curie temperature of the as-quenched material. As a result, after the heat treatment the transition from ferromagnetic into paramagnetic state in the amorphous residual phase can be observed at temperatures close to room temperature. Absence of silicon in the present specimen ensures that only α-Fe phase appears during the first crystallization step which, in turn, essentially simplifies the interpretation of the Mössbauer spectra.

2. Experimental details

Ribbons of the amorphous $Fe_{73.5}Nb_{4.5}Cr_5CuB_{16}$ alloy (width about 1 cm, thickness about 25 μm) were prepared by a rapid solidification from the melt using the melt-spinning technique at the Institute of Physics, Slovak Academy of Sciences in Bratislava. Pieces of ribbons were annealed under an argon protective atmosphere for 1 hour at 550 °C.

The study of the crystallization process of the amorphous precursor was made by means of DSC; the thermal data were collected by a Perkin Elmer DSC-7 unit with the heating rate of 10 K min^{-1}. Magnetic measurements were performed by using vibrating sample magnetometry (VSM) in a temperature range 4.2–800 K.

^{57}Fe Mössbauer experiments were carried out in transmission geometry with a ^{57}Co(Rh) source kept at room temperature. The measurements were performed in the temperature range 5–475 K. The ribbons were placed in an Oxford Instruments bath cryostat, and in a vacuum cryofurnace for below- and above-room-temperature measurements, respectively. An external magnetic field oriented parallel ($H_{ext} \approx 0.05$ T) and perpendicular ($H_{ext} = 4$ T) to the absorber plane was applied. During the high-field experiments the temperature of the source and the absorber was the same, i.e. 65 and 250 K. Evaluation of the hyperfine

spectral parameters was done according to the procedure described in more detail elsewhere [16]. The isomer shift values are related to the centre of an α-Fe calibration Mössbauer spectrum measured at room temperature.

3. Results of the DSC and magnetic measurements

Crystallization stages for the as-quenched $Fe_{73.5}Nb_{4.5}Cr_5CuB_{16}$ alloy are characterized by two endothermic dips positioned in a DSC thermogram at about 525 °C (the first crystallization step), and at about 700 °C (the second one). The first crystallization step starts at $T_{x1} = 480$ °C and corresponds to the formation of bcc Fe phase as confirmed by both x-ray [18] and Mössbauer effect data. The second DSC peak is associated with the crystallization of the residual amorphous matrix. Preparation of the nanocrystalline samples was done at the temperature of 550 °C where the crystallization is already well developed.

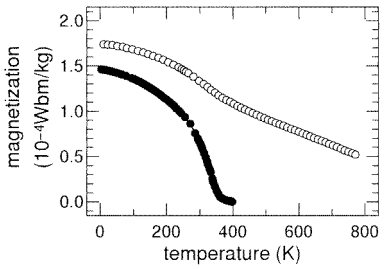

Figure 1. Temperature dependence of saturation magnetization for the $Fe_{73.5}Nb_{4.5}Cr_5CuB_{16}$ alloy: (●) as-quenched, (○) annealed at 550 °C for 1 hour.

Figure 1 shows the temperature dependences of magnetization for amorphous as-quenched and nanocrystalline (550 °C/1 hour) samples measured at an applied field of 0.4 T by using VSM. The magnetization of the as-quenched sample vanishes at $T_c(\mathrm{AM}) = 349$ K, which corresponds to the Curie temperature of the amorphous material. The experimental curve for the nanocrystalline sample shows behaviour typical for material containing two ferromagnetic phases. The clearly visible kink is observed in the temperature range, where the residual amorphous matrix goes from ferromagnetic to paramagnetic state. Above this temperature range, the ferromagnetic Fe-rich nanocrystals exist within the paramagnetic amorphous residue. The Curie temperature for nanocrystalline phase exceeds considerably the maximum measuring temperature, therefore, it was not detected.

In the temperature range below the Curie temperature of amorphous residual matrix, both constituent phases contribute to the magnetic moment of the nanocrystalline sample. As the VSM measurements can provide us only with the overall magnetic moment of such a heterogeneous system, this technique is not suitable for obtaining more detailed information on magnetism of individual phases. Therefore, to obtain better insight into the development of magnetic microstructure with measuring temperature, the Mössbauer spectrometry has been employed.

4. Mössbauer spectrometry for the $Fe_{73.5}Nb_{4.5}Cr_5CuB_{16}$ alloy

4.1. The as-quenched state

Mössbauer spectra for the $Fe_{73.5}Nb_{4.5}Cr_5CuB_{16}$ as-quenched alloy taken at 77 and 295 K are shown in figure 2. Their corresponding hyperfine field values $P(H)$ are given on the right-hand side of the same figure. The decomposition of the $P(H)$ distributions into Gaussian components is plotted by dotted lines.

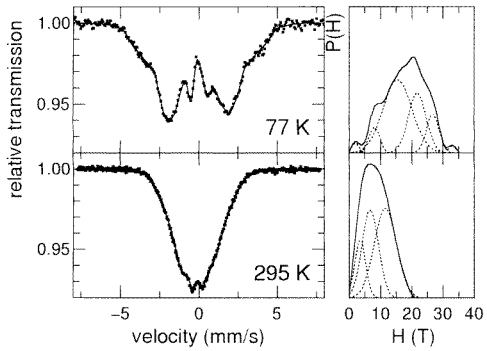

Figure 2. Mössbauer spectra (left) taken at 77 K ($H_{ext\|} = 0.05$ T) and 295 K, and the corresponding distributions of hyperfine fields (right) of the as-quenched $Fe_{73.5}Nb_{4.5}Cr_5CuB_{16}$ alloy. Decompositions of the $P(H)$ distributions into Gaussian components are plotted in dotted lines.

The room-temperature spectrum exhibits a broad-line pattern characteristic of atomic arrangements with mixed electric quadrupole and magnetic dipole interactions and its asymmetric hyperfine magnetic field distribution is shifted towards low H-values. The average value of the $P(H)$ distribution and of the isomer shift (with respect to a room-temperature Mössbauer spectrum of α-Fe) is (8.56 ± 0.03) T, and (-0.04 ± 0.03) mm s^{-1}, respectively. A complex hyperfine field structure is routinely observed in Cr-containing metallic glasses [19, 20]. With the aim to shed some light on the nature of hyperfine interactions and/or short-range order we have measured the $Fe_{73.5}Nb_{4.5}Cr_5CuB_{16}$ as-quenched alloy at 77 K which is well below its ordering temperature ($T_C = 349$ K).

The spectrum taken at 77 K exhibits a distinguishable distributed sextet which implies a presence of magnetic interactions. However, small satellite peaks on both sides of the main $P(H)$ peak in the top right-hand side of figure 2 suggest significant deviations in atomic arrangements from the point of view of the short-range order. Consequently, hyperfine interactions of different origin are evident. This assumption is supported by the character of the main peak which features 'shoulders' towards low H-values (the Gaussian components positioned at about 8 and 15 T with the relative fraction of 7% and 52%, respectively). We have recorded the 77 K Mössbauer spectrum in an external magnetic field of 0.05 T oriented perpendicular to the direction of the γ beam, i.e., parallel with the plane of the ribbon-shaped absorber, to ensure that the satellite $P(H)$ peaks (the Gaussian components at 2 and 33 T which contribute by about 2 and 1%, respectively) are not artefacts due to the fitting method used. Such an experimental arrangement guarantees that all of the individual magnetic moments within the magnetically soft sample are aligned into the plane of the ribbon. This in turn simplifies the fitting procedure because the line intensity ratio can be fixed to 3:4:1:1:4:3, and, consequently, one of the sources of possible misinterpretations

is reduced. The average value of the hyperfine field distribution and of the isomer shift derived from the Mössbauer spectrum at 77 K is (17.9 ± 0.1) T and $(+0.10 \pm 0.06)$ mm s^{-1}, respectively.

4.2. The nanocrystallized state

Mössbauer spectra for the $Fe_{73.5}Nb_{4.5}Cr_5CuB_{16}$ alloy annealed at 550 °C for 1 hour and then taken at 77 and 295 K are shown in figure 3 as examples of the spectrum refinement. The experimental data were fitted by separate independent blocks of hyperfine field distributions assigned to the amorphous residual phase (AM) and to the interface zone (IF). The latter represents Fe atoms situated in crystal grain boundaries as well as Fe atoms in the nanocrystal-to-amorphous interface region that originate from the amorphous precursor and are in close contact with the nanocrystalline grains. A discrete sextet of Lorentzian lines was used to stand for the crystalline component (CR).

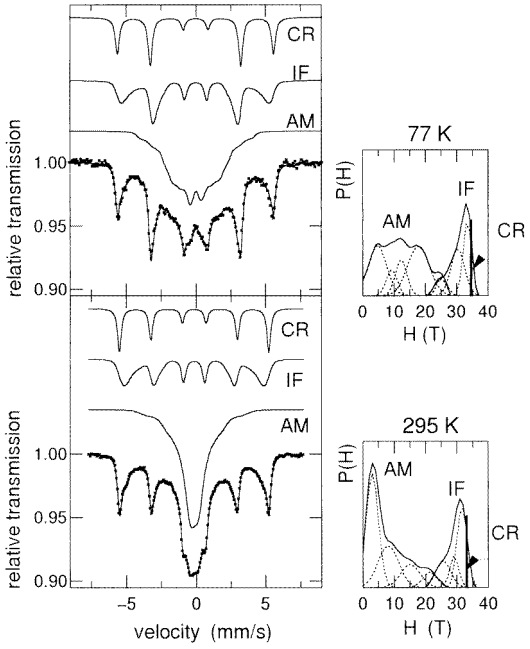

Figure 3. Mössbauer spectra (left) taken at 77 and 295 K, and the corresponding distributions of hyperfine fields (right) of the 550 °C/1 h heat-treated $Fe_{73.5}Nb_{4.5}Cr_5CuB_{16}$ alloy. Partial subspectra for the crystalline phase—CR, interface zone—IF, and amorphous residual phase—AM—are drawn separately. Decompositions of the $P(H)$ distributions into Gaussian components are plotted in dotted lines. The thick vertical line, which stands for the hyperfine field of the CR subspectrum, is scaled down by a factor of five.

Generally speaking, the limits of distribution blocks are governed by spectral line overlap (taking into account also the texture effects) which can yield artificial peaks in $P(H)$ distributions because of contributions from the second and fifth lines of the individual sextets. Indeed, such a situation was recently reported: though the interfacial regions were considered the spectrum evaluations have been made by single-block $P(H)$ distributions with non-physical peaks resulting from the fitting procedure [21]. Because of the extended

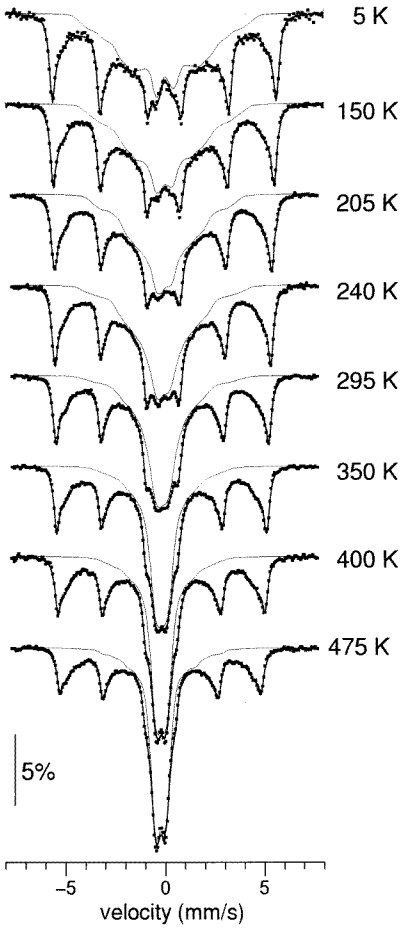

Figure 4. Mössbauer spectra taken at the temperatures indicated of the 550 °C/1 h heat-treated $Fe_{73.5}Nb_{4.5}Cr_5CuB_{16}$ alloy. Subspectra belonging to the amorphous residual phase are plotted in thin solid lines.

range of hyperfine interactions found within nanocrystalline alloys ($0 \rightarrow 36$ T) and usual spectral line overlap the two-block distribution model is superior to a single-block one [16].

For the sake of clarity, the individual subspectra are drawn in figure 3 in separation from the experimental points and the resulting theoretical curve. Their corresponding hyperfine field values $P(H)$ are given on the right-hand side of the same figure. The thick solid vertical lines, which are scaled down by a factor of five with respect to the distribution's $P(H)$ axis, represent discrete hyperfine fields of the CR phases. The decomposition of the $P(H)$ distributions into Gaussian components is plotted by dotted lines. As in figure 2, they are present to illustrate an analysis of $P(H)$ from the point of view of magnetically different Fe sites within the particular phase. A more detailed description regarding the fitting procedure can be found elsewhere [16].

According to the spectral parameters [22], the sextet of Lorentzian lines is unambiguously attributed to the bulk of α-Fe nanocrystalline grains for both spectra. The room-temperature Mössbauer spectrum in the bottom part of figure 3 shows a dominant broad central feature. It can be assigned to the AM part of the $Fe_{73.5}Nb_{4.5}Cr_5CuB_{16}$

nanocrystalline sample whose hyperfine field values extend from 0 up to 27 T. The outweighing $P(H)$ component located at about 3 T which contributes by 48% to the AM $P(H)$ distribution (i.e., by about 27% to the total spectrum) implies that a significant role is played by electric quadrupolar interactions due to the Nb and Cr enrichment inside the amorphous residual phase.

The Mössbauer spectrum in figure 3 taken at 77 K was recorded in external magnetic field oriented parallel with the ribbon's plane to ease the fitting procedure. Hyperfine interactions with higher H-values ($\sim$18 T) become more important ($\sim$21 and 38%, respectively) which leads to subsequent broadening of the AM subspectrum. Closer insight into the nature of hyperfine interactions in the AM and IF subspectra is provided in section 4.4.

Figure 4 illustrates the evolution of Mössbauer spectra for the $Fe_{73.5}Nb_{4.5}Cr_5CuB_{16}$ nanocrystalline alloy with proceeding temperature of measurement. The AM subspectra plotted in thin solid lines clearly demonstrate a continuous conversion of dominating magnetic interactions, which are observed as noticeably broad spectral lines extended over a wide velocity range at low temperatures ($T < 205$ K), into a prevailing paramagnetic spin arrangement characterized by a central doublet at high temperatures of measurement ($T > 295$ K).

4.3. The spectral parameters

The spectral parameters comprising the isomer shift values, the average values of hyperfine fields and the relative fractions of the spectral components are plotted against temperature of measurement in figure 5 by solid circles for the AM phase; open circles stand for the IF region, and open triangles denote the CR phase.

As evident from figure 5(a), the isomer shifts (with respect to a Mössbauer spectrum of α-Fe at room temperature) are very alike for all phases over the whole temperature range. Moreover, they match perfectly with those for α-Fe taken from [22] which we have normalized according to the value of -0.12 mm s^{-1} reported for 294 K. Figure 6(a) shows the comparison between bulk α-Fe data from [22] (plotted by solid triangles) and the CR nanocrystalline phase (open triangles).

The temperature dependence of the AM average hyperfine field (solid circles in figure 5(b)) suggests that the ferromagnetic-to-paramagnetic transition does not proceed over the whole AM bulk at the same temperature. A single T_C(AM)-value cannot be determined; some iron nuclei still exhibit a high magnetic hyperfine field, whereas others are paramagnetic, according to their respective neighbourhoods.

The temperature dependences for the IF and CR average hyperfine fields (open circles and triangles in figure 5(b), respectively) decline even more moderately, a feature which is characteristic for crystalline phases in the displayed temperature range. They are compared with the hyperfine fields of α-Fe in figure 6(b). The values for α-Fe taken from [22] are given in solid triangles. The size of the nanocrystals in the present $Fe_{73.5}Nb_{4.5}Cr_5CuB_{16}$ alloy annealed for 1 hour at 550 °C was determined to be 4–8 nm and 8 nm from a transmission electron micrograph [15], and from a x-ray diffractogram [18], respectively. These small grain dimensions and sufficiently thick intergranular matrix with considerable paramagnetic fraction are supposed to be responsible for the observed differences. Lower values for the IF component with respect to the CR one can be explained by a disordered arrangement of the IF atoms and their neighbourhoods in grain boundaries.

A superparamagnetic behaviour of the ensemble of nanocrystalline particles was recently confirmed at high temperatures for $Fe_{66}Cr_8CuNb_3Si_{13}B_9$ [23] and $Fe_{72}CuNb_{4.5}Si_{13.5}B_9$

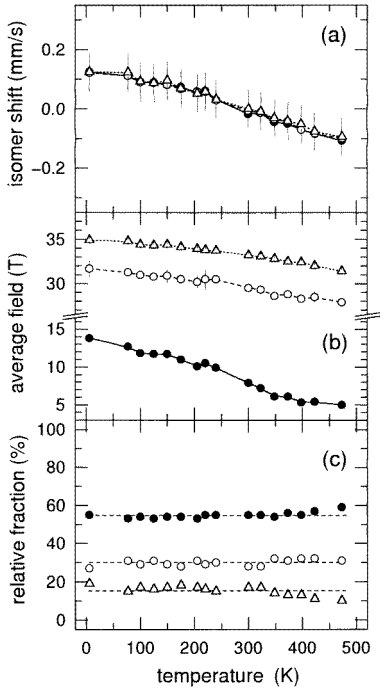

Figure 5. Parameters of the Mössbauer spectrum components (●) AM, (○) IF, (△) CR plotted against the temperature of measurement for the 550 °C/1 h heat-treated $Fe_{73.5}Nb_{4.5}Cr_5CuB_{16}$ alloy: the isomer shift (a), the average field (b) and the relative fraction (c).

[24, 25] alloys using magnetic measurements. At elevated temperatures of measurement, thick paramagnetic layers minimize the dipolar magnetic interactions among ferromagnetic nanocrystals. As a consequence, a decrease in H_{eff} is observed in the CR component with respect to the H_{eff} value of pure α-Fe at temperatures where the AM phase is not fully magnetic. One can suggest that superparamagnetic behaviour of the α-Fe nanoparticles could contribute to the more rapid decrease of the hyperfine field of the CR component as compared to the bulk α-Fe and to the broadening of lines. However, in-field high-temperature Mössbauer experiments (350 K $< T <$ 400 K) have to be performed to check that superparamagnetic behaviour is occurring. Nevertheless, the fraction of the crystalline phase in the present sample, i.e. small intergrain distances, prevent superparamagnetic effects within this temperature range.

The CR H-values in figure 6(b) are intercepting those of pure bulk bcc Fe showing higher and lower values at low and high temperatures, respectively. We propose the following possible explanation based on the differences in density of packing of the atoms located inside the grains (CR phase) and atoms of the grains' surfaces (IF), which are in close contact with the AM phase. Indeed, changes in the volume expansion are expected in the course of nanocrystallization because densities of crystalline and amorphous states are different. During the changes in the temperature of measurement, internal stresses might be generated, which could affect the value of hyperfine fields of surrounding atoms. In the case of iron, an expansion of the nearest-neighbour spacing is expected to result in an enhanced magnetic moment per atom (Bethe–Slater curve) and, consequently, in an observed enhanced hyperfine field.

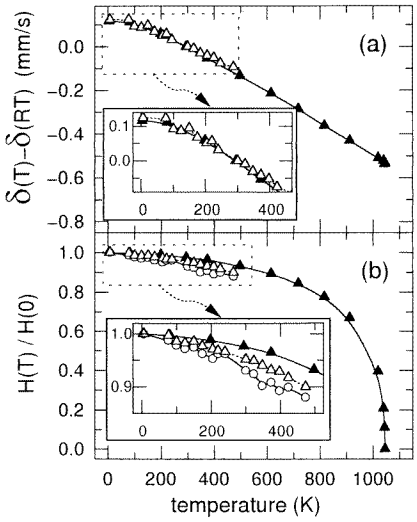

Figure 6. Parameters of the Mössbauer spectrum components (○) IF and (△) CR plotted against the temperature of measurement for the 550 °C/1 h heat-treated $Fe_{73.5}Nb_{4.5}Cr_5CuB_{16}$ alloy: the isomer shift (a), and the hyperfine field (b) as compared with the data (▲) taken from [22].

The relative fractions of spectral components are drawn in figure 5(c). Under the assumption of equal f-factors for each Fe site, they were determined to be 55%, 30% and 15% for the AM, IF and CR phase, respectively. Deviations from these values observed in figure 5(c) stem from the fitting procedure, during which we have not involved any constraints regarding the contributions of individual subspectra at different temperatures of measurements. Statistical evaluation of the relative fractions for all measuring temperatures yields the highest standard deviation and error of 2.5% and ±0.6%, respectively. It is noteworthy that the relative amount of crystalline phase in the $Fe_{73.5}Nb_{4.5}Cr_5CuB_{16}$ alloy annealed at 550 °C for 1 hour was reported to be of about 55% as derived from x-ray measurements [18]. This is in fairly good agreement (3σ-range) with the present results which give the total relative area of spectral components related to the nanocrystals $A(\mathrm{IF}+\mathrm{CR}) \approx 45\%$. The IF phase contains also Fe atoms located in the surface of nanocrystalline grains which are difficult to distinguish by x-ray diffraction.

If we assume that the nanocrystalline grains are spherical in shape with a diameter $d \approx 8$ nm, we can estimate the effective thickness t of the interface zone (surface layer of the grains) from the relation $(A(\mathrm{IF})+A(\mathrm{CR}))/A(\mathrm{CR}) \approx (1+2t/d)^3$ to be about 1.5 nm. It is noteworthy that the latter value was obtained using the upper limit of the grain's size as well as the given fractions of the respective spectral components. Thus, the interface zone is extended over about two atomic layers.

4.4. The distributions of hyperfine fields

Mössbauer spectrometry offers an unique opportunity to study the hyperfine field distributions of the resonating nuclei positioned at different structural neighbourhoods. In the case of a nanocrystalline two-phase system, along with the CR grains, it is the intergranular amorphous remainder, and, especially, the interface zone which are in the centre of research

activities. The present fitting method provides us with both the AM and the IF $P(H)$ distributions as already documented in figure 3.

The hyperfine field distributions from all Mössbauer spectra have been compiled together according to the temperature of measurement. No smoothing procedure was applied. The obtained three-dimensional (3D) $P(H)$ mappings in figure 7 display the evolution of hyperfine interactions for the AM and IF parts of the $Fe_{73.5}Nb_{4.5}Cr_5CuB_{16}$ nanocrystalline alloy. The scales on the $P(H)-$, and temperature-axes, as well as the range of H-values, are the same to allow a straightforward qualitative and quantitative comparison. Contour plots are also given in the bottom part of figure 7.

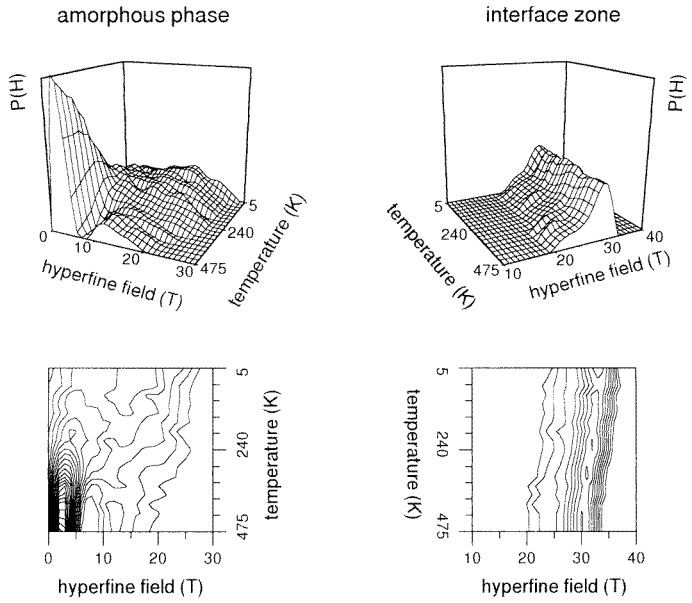

Figure 7. Three-dimensional mappings (top), and the contour plots (bottom) of the hyperfine magnetic field distributions $P(H)$ for the 550 °C/1 h heat-treated $Fe_{73.5}Nb_{4.5}Cr_5CuB_{16}$ alloy corresponding to the amorphous residual phase (left) and to the interface zone (right). The temperature of measurement is the second dimension.

The 3D IF $P(H)$ mapping on the right-hand side of figure 7 does not show substantial changes in the character of hyperfine magnetic fields with the temperature of measurement. As expected, the position of the main $P(H)$ hump is shifted towards lower H-values with rising temperature. This behaviour is clearly seen on the corresponding contour plot and coincides with the temperature dependence of the hyperfine fields in figure 5(b) (open circles). The interface zone consists of Fe atoms located in the nanocrystalline grains' surfaces, and in the peripheral part of the amorphous matrix which is in close contact with the crystallites. The former exhibit hyperfine field values close to that of the CR α-Fe phase and they belong to the higher IF $P(H)$ hump whereas the latter Fe atoms experience more structurally and chemically heterogeneous nearest neighbours and that is why their hyperfine magnetic fields are assigned to the lower IF $P(H)$ hump.

A notable change in the character of magnetic interactions with rising temperature of measurement is revealed in the 3D AM $P(H)$ mapping. Segregation of Fe atoms into bcc Fe grains leaves behind regions enriched in other constituent elements, namely Nb and Cr. Using atom-probe field ion microscopy, and high-resolution transmission electron

microscopy combined with nanobeam electron diffraction, it was concluded that Zr is segregated to the remaining amorphous phase just near the interface, and the concentration profiles for Zr and B constituent elements are significantly enriched at the interface between bcc Fe and amorphous phases in nanocrystalline FeZrBAl, FeZrBSi and FeZrB alloys [26]. A similar situation can be considered to take place in the $Fe_{73.5}Nb_{4.5}Cr_5CuB_{16}$ nanocrystalline alloy. Regions with higher Nb and Cr content will transform into a paramagnetic state at lower temperature than in the original as-quenched alloy. The prevailing influence of Fe atoms with Nb and Cr nearest neighbours can be seen in the left-hand side of figure 7 already at $T \approx 240$ K by a sharp and well developed hump located at about 3 T.

On the other hand, the magnetic interactions which are represented by humps positioned at about 9, 15 and 21 T (at 77 K) are gradually vanishing. Eventually, only minute traces of small magnetic hyperfine fields ($\approx$13 T) remain at 475 K. The shift of hyperfine fields toward low H-values as well as a growth of the dominating component, which in fact represents electric quadrupole interactions, can be easily followed on the contour plot drawn in the bottom part of figure 7.

Using the 3D AM $P(H)$ mapping it is possible to explain also the behaviour of the temperature dependence of the average hyperfine field of the AM phase in figure 5(b) (solid circles). Transition from magnetic into a paramagnetic state does not take place uniformly in the whole AM matrix. Instead, regions with different topological and/or chemical short-range orders exist which manifest themselves through hyperfine interactions of different nature. Consequently, the whole AM phase can be decomposed into paramagnetic and weak magnetic areas. As a result, a single value of magnetic ordering temperature cannot be determined.

4.5. Paramagnetic and weak magnetic regions inside the amorphous remainder

Let us examine the room-temperature Mössbauer spectrum of the $Fe_{73.5}Nb_{4.5}Cr_5CuB_{16}$ nanocrystalline alloy presented in figure 3 (bottom part): the subspectrum due to the AM component exhibits a central broad line superimposed on another broadened feature giving rise to a complex hyperfine structure originating from the simultaneous presence of both quadrupolar electric and dipolar magnetic interactions. It is frequently observed that the hyperfine structure and magnetic properties of amorphous alloys strongly depend on the Nb [18, 27] and/or Cr content [19, 20, 28]. The analysis of the 3D $P(H)$ mappings given above also suggests that a heterogeneous content of Fe and Cr occurs within the AM phase in the present nanocrystalline alloy. Subsequently, a superior fitting model to a subspectrum due to the AM component would introduce a decomposition of the AM distribution block into two parts.

Figure 8 shows two approaches to fit the Mössbauer spectrum for the $Fe_{73.5}Nb_{4.5}Cr_5CuB_{16}$ nanocrystalline alloy measured at 400 K where the dominating contribution of electric quadrupole interactions is obvious. The spectrum was first analysed using the fitting procedure discussed in section 4.2. The results of fit I are presented in the upper part of figure 8. A pronounced peak in the $P(H)$ corresponding to the AM phase is localized at about 3.5 T. It indicates a collapse of ferromagnetic exchange interactions in a certain portion of the amorphous residual phase and should be ascribed to prevailing quadrupolar electric interactions. Such an experimental feature reinforces the heterogeneous chemical character of the amorphous matrix.

For that reason, we have adopted another procedure (fit II) which consisted in replacing the low magnetic fields of the AM $P(H)$ by a quadrupolar component. In other words, we

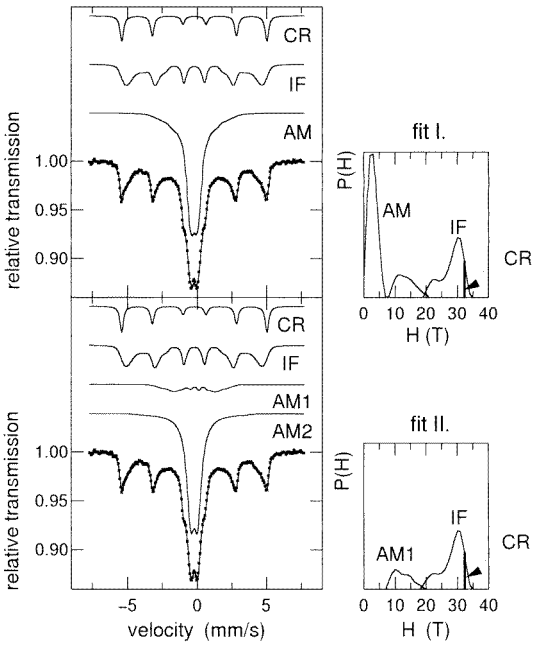

Figure 8. Mössbauer spectra (left) taken at 400 K, and the corresponding distributions of hyperfine fields (right) of the 550 °C/1 h heat-treated $Fe_{73.5}Nb_{4.5}Cr_5CuB_{16}$ alloy, as obtained from different fitting models (see the text). The thick vertical line, which stands for the hyperfine field of the CR subspectrum, is scaled down by a factor of five.

have decomposed the original subspectrum due to the AM phase into two components AM1 and AM2 which are restored using a distribution of magnetic sextets and an asymmetrical quadrupolar doublet with broad Lorentzian lines, respectively. Because we have used the NORMOS DIST program version 1989 which allows treatment of only two distribution blocks of the same nature (magnetic fields or quadrupolar splitting) the distribution of quadrupolar splitting in fit II was modelled by a broadened doublet of Lorentzian lines; the ratio of line intensities of the doublet, D_{21}, was free during the fitting procedure to account for its possible asymmetry. The Mössbauer spectrum with all these components as well as hyperfine fields corresponding to the AM1, IF, and CR phases are illustrated in the bottom part of figure 8.

The spectral parameters derived from the Mössbauer spectra tailored to fit II over the temperature range where the central doublet is dominant are shown in figure 9 for the amorphous phase (AM1 and AM2), the interface zone IF and the α-Fe crystalline component CR. The isomer shift values in figure 9(a) as well as the IF and CR average hyperfine fields in figure 9(b) exhibit the same temperature dependences as those for fit I in figure 5(a) and 5(b), respectively. The character of the average field in the AM1 component, i.e. in the magnetic part of the amorphous residual phase, exhibits only shallow decrease with rising temperature of measurement which implies a rather high value of T_C(AM1). The average 'hyperfine fields' for the paramagnetic AM2 phase were obtained from the corresponding quadrupole splitting values by calculation and they are shown just for the sake of comparison. Relative fractions for the IF and CR phases in figure 9(c) are almost unchanged (within the statistical error) in relation with those from the fit I. Towards the high-temperature range

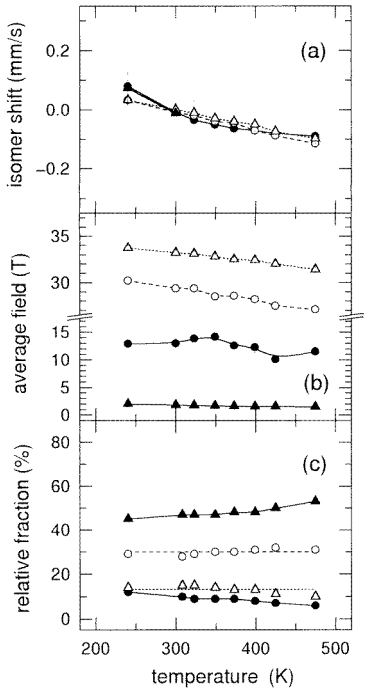

Figure 9. Parameters of the Mössbauer spectrum components derived from the fit II (see the text) (●) AM1, (▲) AM2, (○) IF, (△) CR plotted against the temperature of measurement for the 550 °C/1 h heat-treated $Fe_{73.5}Nb_{4.5}Cr_5CuB_{16}$ alloy: the isomer shift (a), the average field (b) and the relative fraction (c).

of measurement, an increase in the AM2 content (doublet of the paramagnetic amorphous remainder) is observed on account of the magnetic amorphous AM1 fraction.

The full line width, the quadrupole splitting and the intensity ratio of the first and the second line, D_{21}, of the AM2 doublet in figure 10 implies that with rising temperature of measurement the paramagnetic amorphous region shows a tendency towards higher short-range order arrangement. This assumption is supported mainly by a considerable decrease in the line width.

3D mappings of AM1 and IF $P(H)$ distributions as obtained from the fit II are demonstrated in figure 11. The same scales allow their mutual comparison. Changes in the magnetic microstructure of the amorphous residual phase (AM1 in figure 11 (left)) correspond to a weakening of the magnetic interactions with increasing temperature of measurement. This conclusion is based on the fact that the high-field $P(H)$ peak located at about 17 T at 275 K is notably shifted towards lower field values with rising temperature of measurement and eventually it completely vanishes. On the other hand, the IF $P(H)$ distributions in figure 11 (right) depict a formation of a hump positioned at about 18 T at 475 K. This can be interpreted in terms of temperature-based decrease of magnetic hyperfine fields (note that the main as well as the satellite humps in figure 11 (right) are shifted towards lower fields with rising temperature of measurement) but also changes in the magnetic microstructure inside the AM phase should be taken into consideration.

The slow temperature evolution of the central part of the Mössbauer spectra clearly shows a progressive increase of the paramagnetic contribution of the residual amorphous

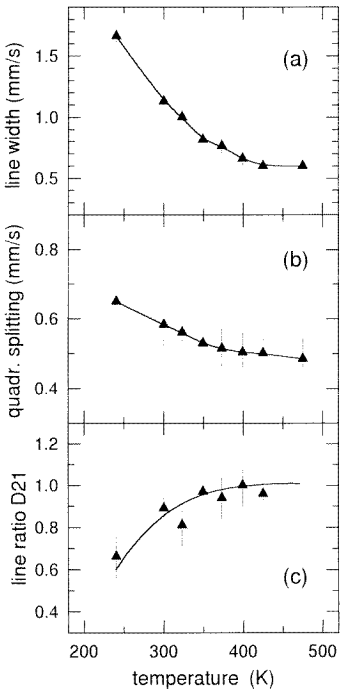

Figure 10. Parameters of the paramagnetic doublet AM2 from fit II to the Mössbauer spectra of the 550 °C/1 h heat-treated $Fe_{73.5}Nb_{4.5}Cr_5CuB_{16}$ alloy plotted against the temperature of measurement: the line width (a), the quadrupole splitting (b) and the line intensity ratio D_{21} (c).

phase, i.e. the number of paramagnetic Fe moments. The fit II, however, has some shortcomings which are related to line overlap of the spectral components attributed to the magnetic and non-magnetic amorphous residual phases. Consequently we propose a further fitting procedure, fit III, which consists in introducing in addition to sextets assigned to both crystalline, magnetic amorphous phases and interface, a paramagnetic quadrupolar component keeping its intensity free. Indeed, we assumed that the resulting quadrupolar component should exhibit a hyperfine structure which is roughly similar to that observed in the as-quenched state, in contrast to the magnetic hyperfine structure which is strongly different, because the iron content of the amorphous residual phase has been strongly reduced during the first stage of crystallization. Such an approach aims to point another direction in searching for proper description of complex demonstration of hyperfine interactions.

The fit III procedure was started by recording paramagnetic Mössbauer spectra of the as-quenched sample at several temperatures: no changes were observed in the temperature range 400–600 K, except the isomer shift value. These spectra were reproduced by means of a discrete distribution of quadrupolar splitting linearly correlated to that of an isomer shift. The fitting procedure of the Mössbauer spectra recorded on the present nanocrystalline alloys was performed assuming three sextets attributed to the crystalline grains, the interface and the amorphous residual phase and a quadrupolar doublet. This latter component, only the proportion of which was refined, results from the discrete distribution of the quadrupolar splitting similar to that deduced from as-quenched paramagnetic spectra, correlated to the same isomer shift, but the average value of that distribution was assumed to be temperature dependent according to the results obtained on the as-quenched sample.

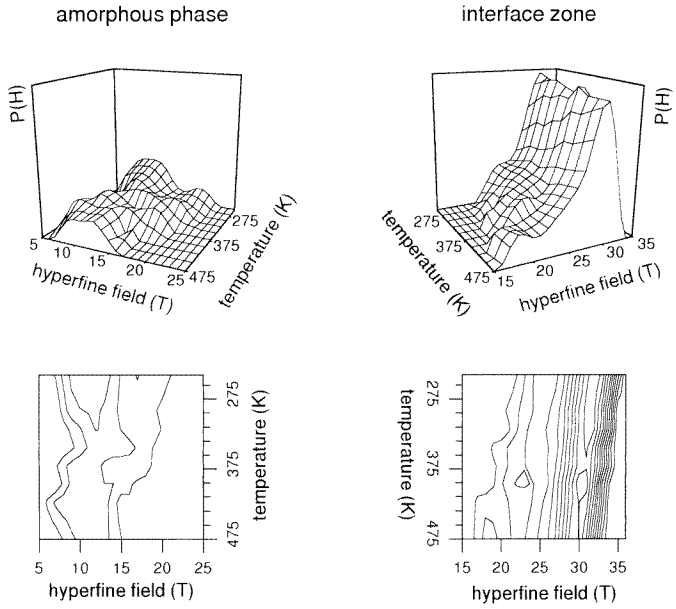

Figure 11. Three-dimensional mappings (top), and the contour plots (bottom) of the hyperfine magnetic field distributions $P(H)$ derived from fit II to the Mössbauer spectra of the 550 °C/1 h heat-treated $Fe_{73.5}Nb_{4.5}Cr_5CuB_{16}$ alloy corresponding to the amorphous residual phase (left) and to the interface zone (right). The temperature of measurement is the second dimension.

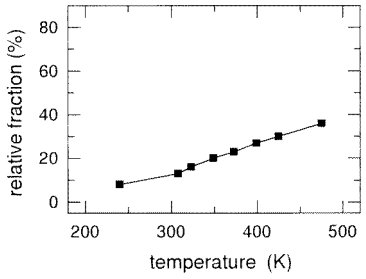

Figure 12. Relative fraction of a paramagnetic doublet from fit III plotted against the temperature of measurement.

The proportion of the quadrupolar component progressively increases with temperature as is shown in figure 12. This behaviour may be explained by the segregation of Nb atoms close to the grains, and consequently a lower Fe content, which both progressively evolve to the expected composition of the residual amorphous phase, far from the crystalline grains. However, the temperature spread of the collapse of the magnetic sextet into a quadrupolar doublet cannot only be due to the non-homogeneous composition. Accounting for the size of the grains and the high volume fraction of the crystalline phase, one can expect rather short distances between the crystalline grains (2–4 nm) and a composition with low Fe content of the residual amorphous phase, consistent with a paramagnetic state occurring at low temperatures: consequently, one suggests that the presence of strong exchange interactions

between grains can penetrate the intergranular phase over 1–2 nm thickness, that would induce small values of hyperfine field at Fe atoms located within the residual amorphous phase, which decrease with increasing temperatures.

4.6. Mössbauer spectra in a perpendicular external magnetic field

We have used an external magnetic field $H_{ext} = 4$ T oriented perpendicular to the absorber's plane, i.e. parallel with the γ-beam direction. Such geometry and field intensity ensure that all magnetic moments within the nanocrystallized sample are aligned into the direction of the external magnetic field, i.e. normal to the ribbon plane. As a result, the transitions $\Delta m = 0$ disappear and a fixed Mössbauer spectrum line intensity ratio of 3:0:1:1:0:3 can be applied during the fitting procedure. Such an approach not only simplifies the evaluation procedure by eliminating the effects of line overlap but also equalizes the magnetic texture.

Mössbauer spectra for the $Fe_{73.5}Nb_{4.5}Cr_5CuB_{16}$ nanocrystal taken at the temperatures of 65 K and 250 K are illustrated in figure 13. During these experiments, the source was also kept at the indicated temperature to minimize the consumption of liquid helium. The AM subspectra show a dominating central part which indicates that paramagnetic regions occur in the amorphous remainder already at the low temperature of 65 K. This was not observed to such extent in out-of-field experiments. At 250 K, the contribution of magnetic regions is more suppressed and the separation of non-magnetic and magnetic spectral components is more evident.

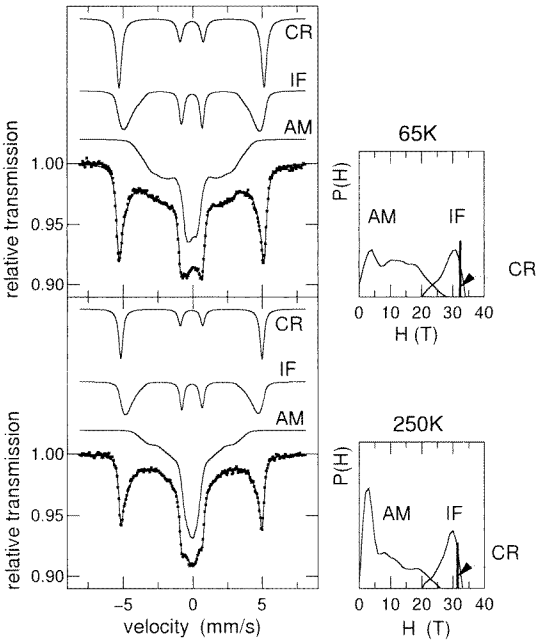

Figure 13. Mössbauer spectra (left) taken at 65 and 250 K in an external magnetic field ($H_{ext} = 4$ T) oriented perpendicular to the absorber's plane, and the corresponding distributions of hyperfine fields (right) of the 550 °C/1 h heat-treated $Fe_{73.5}Nb_{4.5}Cr_5CuB_{16}$ alloy. Partial subspectra for the crystalline phase—CR, interface zone—IF—and amorphous residual phase—AM—are drawn separately. The thick vertical line, which stands for the hyperfine field of the CR subspectrum, is scaled down by a factor of five.

5. Conclusions

The extended Mössbauer effect study performed on the $Fe_{73.5}Nb_{4.5}Cr_5CuB_{16}$ nanocrystal (annealed at 550 °C for 1 hour) over a wide temperature range together with the magnetic and DSC measurements provide the following conclusions:

(1) The crystalline phase was identified to be α-Fe. The hyperfine field values, however, are lower at elevated temperatures of measurements than the expected ones, but they are also higher at low temperatures according to our results. The presence of impurities in nanocrystalline grains as proposed by Vincze *et al* [29] has been considered but it does not describe the low-temperature anomalies. Our interpretation of such behaviour as mentioned in the text provides another possible answer. Further research on this interesting topic is in progress.

(2) For the as-quenched sample, the T_C was determined to be about 350 K. The transition from ferromagnetic to paramagnetic state of the amorphous residual phase proceeds within a broad temperature interval and that is why it is not possible to determine a single value of the magnetic ordering temperature.

(3) Three-dimensional mappings of the hyperfine field distributions exhibit a presence of atoms with different topological and/or chemical short-range orders both inside the amorphous and interface zone. As a consequence, paramagnetic, weak magnetic and ferromagnetic regions are observed in the former part of the nanocrystalline alloy.

(4) The fitting procedure employed in the analysis of the Mössbauer spectra consists of two independent blocks of hyperfine field distributions which can be assigned to the amorphous phase and to the interface zone, respectively, and one sextet of Lorentzian lines attributed to the α-Fe nanocrystalline grains. For high measuring temperature, the AM $P(H)$ distribution can be further decomposed into two parts (distribution of hyperfine fields and quadrupole splittings) accounting for the presence of simultaneous magnetic and electric hyperfine interactions.

(5) The results achieved in external magnetic fields oriented parallel and perpendicular to the ribbon plane are fully consistent (see the $P(H)$ shapes for example) with those obtained at different temperatures of the out-of-field measurements.

(6) Relative fractions of the AM, IF and CR parts were determined to be 55, 30 and 15%, respectively. Using the average grain size of 8 nm, the interface zone thickness is estimated at 1.5 nm which is larger than that expected to cover approximately two atomic layers.

In this paper, we have tried to underline the possibilities of Mössbauer spectrometry in the investigation of nanocomposite materials featuring powerful potential in the evaluation of hyperfine interactions (distributions of hyperfine fields). Closer insight into the interface zone was also unveiled and an unmatched role of this technique was pointed out. Still, in order to obtain a complete figure of the magnetic behaviour, the results from Mössbauer effect measurements ought to be correlated with other experiments.

Acknowledgments

The amorphous ribbons were provided by courtesy of Dr P Duhaj. The authors would like to thank Dr J Kováč for his assistance with the VSM measurements. One of us (MM) is thankful to the Region Pays de la Loire for financial support during his stay in Le Mans.

References

[1] Herzer G 1992 *J. Magn. Magn. Mater.* **112** 258–62
[2] Suzuki K, Makino A, Inoue A and Masumoto T 1991 *J. Appl. Phys.* **70** 6232–7
[3] Makino A, Inoue A, Hatani T and Bitoh T 1997 *Mater. Sci. Forum* **235–238** 723–8
[4] Herzer G and Warlimont H 1992 *NanoStruct. Mater.* **1** 263
[5] Würschum R 1995 *NanoStruct. Mater.* **6** 93–104
[6] Ślawska-Waniewska A, Gutowski M, Kuźmiński M, Dynowska E and Lachowicz H K 1994 *Nanophase Materials* ed G C Hadjipanayis and R W Siegel (Dordrecht: Kluwer) pp 721–8
[7] Jędryka E, Randrianantoandro N, Grenèche J M, Ślawska-Waniewska A and Lachowicz H K 1995 *J. Magn. Magn. Mater.* **140–144** 451–2
[8] Randrianantoandro N, Grenèche J M, Jędryka E, Ślawska-Waniewska A and Lachowicz H K 1995 *Mater. Sci. Forum* **179–181** 545–50
[9] Conde C F, Millán M and Conde A 1994 *J. Magn. Magn. Mater.* **138** 314–8
[10] Lin T, Xu Z X and Ma R Z 1996 *NanoStruct. Mater.* **7** 733–40
[11] Hernando A and Kulik T 1994 *Phys. Rev.* B **49** 7064–7
[12] Navarro I, Ortuño M and Hernando A 1996 *Phys. Rev.* B **53** 11 656–60
[13] Miglierini M, Labaye Y, Randrianantoandro N and Grenèche J M 1997 *Mater. Sci. Eng.* A **226–228** 559–64
[14] Miglierini M and Grenèche J M 1997 *Czech. J. Phys.* **47** 507–12
[15] Škorvánek I, Miglierini M and Duhaj P 1997 *Mater. Sci. Forum* **235–238** 771–6
[16] Miglierini M and Grenèche J M 1997 *J. Phys.: Condens. Matter* **9** 2303–19
[17] Miglierini M and Grenèche J M 1997 *J. Phys.: Condens. Matter* **9** 2321–47
[18] Škorvánek I, Duhaj P, Kováč J, Kavečanský V and Gerling R 1997 *Mater. Sci. Eng.* A **226–228** 218–22
[19] Chien C L 1979 *Phys. Rev.* B **19** 81–6
[20] Whittle G L, Campbell S J and Stewart A M 1982 *Phys. Status Solidi* a **71** 245–51
[21] Brzózka K, Ślawska-Waniewska A, Nowicki P and Jezuita K 1997 *Mater. Sci. Eng.* A **226–228** 654–8
[22] Preston R S, Hanna S S and Heberle J 1962 *Phys. Rev.* **128** 2207–18
[23] Ślawska-Waniewska A, Gutowski M, Lachowicz H K, Kulik T and Matyja H 1992 *Phys. Rev.* B **46** 14 594–7
[24] Škorvánek I and O'Handley R C 1995 *J. Magn. Magn. Mater.* **140–144** 467–8
[25] Škorvánek I, Kim C K and O'Handley R C 1995 *Science and Technology of Rapid Solidification and Processing* ed M A Otoani (Dordrecht: Kluwer) pp 309–16
[26] Inoue A, Takeuchi A, Makino A and Masumoto T 1996 *Sci. Rep. RITU* A **42** 143–56
[27] Miglierini M 1994 *J. Phys.: Condens. Matter* **6** 1431–8
[28] Rajaran G, Prasad S, Chandra G, Shingi S N and Krishnan R 1983 *Phys. Lett.* **98A** 57
[29] Vincze I, Kemény T, Kaptás D, Kiss L F and Balogh J 1997 *ICAME'97 (Rio de Janeiro, 1997) Hyperfine Interact.* at press